Induced carbonate dissolution

Impact of brine chemistry in CO_2 foam

Cobos, Jacquelin E.; Sæle, Aleksandra M.; Benjumea, Maria C.; Charro, Monica M.; Søgaard, Erik G.

Published in:
Gas Science and Engineering

DOI (link to publication from Publisher):
10.1016/j.jgsce.2024.205439

Publication date:
2024

Document Version
Publisher's PDF, also known as Version of record

130 (2024) 205439

Contents lists available at ScienceDirect

Gas Science and Engineering

journal homepage: www.journals.elsevier.com/gas-science-and-engineering

Induced carbonate dissolution: Impact of brine chemistry in CO_2 foam

Jacquelin E. Cobos [a,*], Aleksandra M. Sæle [a], Maria C. Benjumea [b], Monica M. Charro [c], Erik G. Søgaard [d]

[a] Department of Physics and Technology, University of Bergen, Norway
[b] Faculty of Mines, Universidad Nacional de Colombia, Medellin, Colombia
[c] Faculty of Engineering in Earth Sciences, Escuela Superior Politecnica del Litoral, Guayaquil, Ecuador
[d] Department of Chemistry and Bioscience, Aalborg University, Copenhagen, Denmark

ARTICLE INFO

Keywords:
CO_2foam
Carbonate dissolution
Rock-fluid-foam
Fluid-foam interactions

ABSTRACT

Foam CO_2might be considered an efficient alternative to reduce gas mobility and produce favorable mobility ratios. It offers significant advantages, particularly in heterogeneous or fractured reservoirs due to its ability to block highly permeable layers or divert the injected fluid from fractures into the matrix. In the present work, a surfactant solution made of different ionic compositions was co-injected into outcrop Edwards Limestone to determine the impact of brine chemistry on carbonate dissolution upon CO_2foam injection. The development in differential pressures (DP) during continuous co-injection of sc-CO_2 and different surfactant solutions (NaCl, NFB, CB) shows that unwanted chemical reactions (dissolution/precipitation) compromise the rock integrity by more acid formation and wormholing. Rock-fluid-foam interactions indicate that the total heat in the rock-fluid-foam systems is 6.9 mJ $NaCl_{foam}$, 19.3 mJ NFB_{foam}, and 37.8 mJ CB_{foam} systems. On the other hand, the total heat for the fluid-foam interactions is 11.5 mJ $NaCl_{foam}$, 12.5 NFB_{foam}, and 20.4 mJ CB_{foam}. The demicellization of the foam formulations could have led to calcite dissolution. The synergy between ITC and core flooding experiments elucidates the impact of the brine chemistry on calcite dissolution during foam-assisted CO_2sequestration at both microscopic and macroscopic scales.

1. Introduction

Carbon capture and storage (CCS) has been recognized as a technology that contributes to the reduction of carbon dioxide CO_2 emissions (Metz et al., 2005). CCS aims to capture CO_2 emissions at their source, transport them to a suitable storage location, and securely store them in suitable geological formations, such as unmineable coal beds, depleted oil and gas reservoirs, and deep saline aquifers (Al-Khdheeawi et al., 2018). Among all the storage options, depleted oil and gas reservoirs can be considered the best option for underground CO_2 storage through CO_2-EOR due to the existence of infrastructure, the wealth of reservoir data, and the revenue of the incremental oil production that offsets the cost of CO_2 capture and transport. Therefore, CO_2-EOR could help to achieve a win-win solution for climate change mitigation goals by storing CO_2 while prolonging the lifetime of a conventional oil field (Eiken et al., 2011; Enick et al., 2012; Motie and Assareh, 2020). Large-scale CO_2 capture projects linked with EOR have been reported in the literature (International Energy Agency, 2015; Ozaki et al., 2015; Orr, 2018). Orr (2018) mentioned that there are 17 large-scale CCUS projects worldwide. Weyburn and Midale oil fields, located in southeast Saskatchewan, Canada are one of the world's largest commercial CO_2-EOR and sequestration operations. A total carbon storage of 40 Mt (30 Mt at Weyburn and 10 Mt at Midale) and incremental oil recovery of 130 million barrels of medium-gravity crude oil over the 25 years of the project is expected (Riding and Rochelle, 2005). Núñez López et al. (2019) developed a dynamic carbon lifecycle analysis (d-LCA) to understand the evolution of the environmental impact (CO_2 emissions) and mitigation (geologic CO_2 storage) associated with CCUS. Those authors found out that a CO_2-EOR project starts with a negative carbon footprint and, years into the project, transitioned into operating with a positive carbon footprint in different scenarios (e.g. continuous gas injection, water alternating-gas). Those authors claimed that the negative carbon footprint period could last longer by operational changes and injection of CO_2 excess from a recycling facility into an underlying or associated saline aquifer for long-term storage. Moreover, the effectiveness of pure CO_2 injection is affected by its intrinsic properties of low density and viscosity that cause gravitational segregation and viscous fingering. Therefore, poor sweep efficiency and reduced storage capabilities are a direct consequence of those flow instabilities (Jian et al., 2019).

* Corresponding author.
E-mail address: Jacquelin.e.mora@uib.no (J.E. Cobos).

https://doi.org/10.1016/j.jgsce.2024.205439
Received 8 March 2024; Received in revised form 30 May 2024; Accepted 28 August 2024
Available online 30 August 2024

A novel method to reduce gas mobility by increasing the apparent viscosity of CO_2 and, therefore, producing a more favorable mobility ratio is by in-situ foam generation. Foam is a dispersion of gas in a liquid, where the gas is separated by thin liquid films called lamella (discontinuous phase) (Farajzadeh et al., 2015). A foaming agent is needed to stabilize the lamella and avoid the coalescence of the gas bubbles. Surfactants are generally used as foaming agents, which application depends on the rock type. Sandstones are predominately negatively charged, thus, anionic surfactants (negatively charged) are suitable for this type of rock due to their low adsorption. The most common anionic surfactant used in foam-EOR applications is alpha olefin sulfonate with 14 to 16 carbons (AOS 14–16). However, anionic surfactants are prone to precipitate in the presence of divalent cations (e.g. Ca^{2+} and Mg^{2+}). Carbonate formations, on the other hand, tend to be predominately positively charged. Thus, non-ionic surfactants (no charge) or cationic surfactants (positively charged) can be used as foaming agents. Non-ionic surfactants could have ethylene oxide ($–CH_2–CH_2O–$)(EO), or sugar-based hydrophilic groups. On the other hand, cationic surfactants could contain nitrogen-functional groups like amine, substituted amine, or diamine. The selection of a suitable surfactant aims for foam stabilization and avoiding its adsorption or retention on the rock surfaces in order to ensure its propagation to large distances from an injection well. CO_2 foam can be generated in situ by injecting gas and brine with a surfactant in alternating slugs (SAG) or simultaneously (co-injection) (Enick et al., 2012; Liu et al., 2005). CO_2 injection in alternating slugs is the preferred method in most field applications to avoid operational challenges (e.g. injectivity issues, and downhole corrosion) (Hoefner and Evans, 1995). On the other hand, co-injection is preferred at the laboratory scale to achieve a steady-state condition of injection and derive foam model parameters (Alcorn et al., 2019).

Apart from reducing the gas mobility, foam is highly advantageous in heterogeneous or fractured reservoirs due to its ability to block high permeable layers or divert the injected fluid from the fracture into the matrix since it increases the gas viscosity and, therefore hinders rapid gas movement through high-permeability layers (Dong et al., 2018). Føyen et al. (2020) observed a 25% enhancement in CO_2 storage capacity due to enhancement of water mobilization at pore level during foam generation. Hence, CO_2-foam can give higher oil recoveries and CO_2 storage capacities than the conventional CO_2-EOR methods because it increases both sweep efficiency and residual gas saturation in the swept region. Even though CO_2-foam is an effective mobility control method, it can alter the carbonate's mechanical properties. Such alterations disrupt the fluid flow within the reservoir, diminish storage capacity, and ultimately storage security. Therefore, the long-term fate of injected CO_2 requires a fundamental understanding of rock-foam chemical interactions (Calabrese et al., 2005).

Several studies regarding dissolution of calcite and calcite-containing rocks have been reported in the literature (Pokrovsky et al., 2005; Luquot and Gouze, 2009; Ellis et al., 2011; Heeschen et al., 2011; Crockford et al., 2014; Peng et al., 2016; Anabaraonye et al., 2019). Nevertheless, only a few of these studies have shown the impact of brine chemistry carbonate dissolution at conditions relevant for geological carbon storage. Pokrovsky et al. (2005) reported dissolution rates of calcite, dolomite, and magnetite as function of salinity ($0.001M \leq [NaCl] \leq 1M$) and different CO_2 partial pressures ($10^{-3.5} \leq pCO_2 \leq 55$ atm). Those authors found that carbonate mineral dissolution rates depend weakly on pCO_2 and are not proportional to the concentration of H_2CO_3. Anabaraonye et al. (2019) also studied calcite dissolution rates using three different CO_2-saturated brines (NaCl, $NaHCO_3$ and multicomponent Na–Mg–K–Cl–SO_4–HCO_3) at reservoir conditions (temperatures up to 373 K and pressures up to 10 MPa). Those brines were selected because NaCl is the most abundant salt component in saline aquifers, $NaHCO_3$ is a minor component in many reservoir brines but a direct participant in the CO_2 acid–base equilibria and simplified multi-component Na–Mg–K–Cl–SO_4–HCO_3 is based on the composition of a Middle Eastern subsurface brine. Anabaraonye and co-authors noticed during batch reactor experiments with a rotating disk technique that the presence of a multi-component brine and NaCl brine showed a slight increase in the dissolution rate compared to pure CO_2-water systems.

Table 1
Ionic composition in mol/m^3 and intrinsic properties of 3.5 wt% NaCl brine, synthetic North Sea formation brine (NFB), and chalk brine (CB). Ionic strength (I_c) in mol/m^3 was calculated based on the ionic concentrations, and the charge of each ion. Density and pH of the brines were measured at ambient temperature (20 °C) with DMA 35 Anton Paar portable density meter apparatus (reproducibility of 0.5 kg/m^3) and a PC 2700 pH meter from Eutech instruments.

	Ionic composition					Intrinsic properties		
	K^+	Mg^{2+}	Na^+	Ca^{2+}	Cl^-	Ic	ρ	pH
NFB	4.7	21.89	995.96	99.92	1064.56	1.28	1050	6.69
NaCl	–	–	684.40	–	684.40	0.68	1030	6.71
CB	–	–	427.79	225	877.79	1.10	1090	6.70

The present research aimed to determine the impact of foam chemistry on carbonate-induced dissolution by co-injection of CO_2 and surfactant solutions with different chemical compositions. CO_2 foam is a proven technology that increases sweep efficiency and decreases CO_2 mobility at different scales (pore to field) (Føyen, 2020). However, the detrimental impact of CO_2 foam on rock dissolution has not been thoroughly studied. Thus, additional research is required to quantify this problem. This work provides a synergy between microcalorimetry and core flooding experiments to investigate CO_2-foam-reservoir interactions and identify structural changes within the core plugs upon CO_2 foam injection.

2. Materials and methods

2.1. Brines

3.5 wt% NaCl, synthetic North Sea formation brine (NFB), and chalk brine (CB) were prepared in the laboratory by mixing reagent grade salts (purity of 99%, provided by VWR chemicals) with deionized water. In the case of 3.5 wt% NaCl, 35 g NaCl was mixed with 1000 g DW. CB was prepared by adding 25 g NaCl and 25 g $CaCl_2$ in 1 L DW. Finally, NFB was made by mixing 67.3 g NaCl, 4.5 g $MgCl_2$, 14.7 g $CaCl_2$, 0.5 g KCl. The surfactant solutions were made by adding 0.5 wt% non-ionic surfactant, SURFONIC L24-22, to either 3.5 wt% NaCl, NFB, or CB. This non-ionic water-soluble surfactant is a linear ethoxylated alcohol ($C_{12-14}EO_{22}$) used previously in a field-scale CO_2 pilot in East Seminole Field, USA (Alcorn et al., 2020) and lab-scale experiments (Føyen, 2020) by the Reservoir Physics group at University of Bergen.

Table 1 lists the ionic strength, and intrinsic properties for the synthetic brines. NaCl was selected because it is the most abundant component in saline aquifers (Anabaraonye et al., 2019), NFB is a simplified multi-component brine based on the composition of a North Sea formation brine (Cobos et al., 2021) and CB has $CaCl_2$ that helps to minimize calcite (chalk) dissolution (Aspenes et al., 2003).

2.2. Rock sample

In this study, Edwards Limestone was used for both core-flooding and microcalorimetry experiments similar to a work from Cobos et al. (2023). This rock has a trimodal pore size distribution with both vugs and microporosity (Tipura, 2008). X-ray Fluorescence (XRF) analysis was used to determine the elemental composition of the rock material in mass %. Table 2 shows the results obtained from the XRF analysis.

Three cylindrical core samples were used for core flooding experiments. The cores were washed gently with tap water to remove debris and lose particles before co-injecting CO_2 and three different surfactant solutions. Dimensions and dry weights of each core were registered

Table 2
X-ray Fluorescence (XRF) analysis of outcrop Edwards Limestone. Particles with a size of <100 μm were used for the analysis and were obtained by crushing and grounding part of the rock material with a ball mill (Cobos et al., 2021).

	Compound						
	SiO_2	P_2O_5	K_2O	CaO	Fe_2O_3	As_2O_3	SrO
Mass %	1.56	0.16	0.07	97.6	0.38	0.09	0.09

Table 3
Core properties.

Core id.	l [cm]	d [cm]	ϕ [%]	k_0 [mD]	PV [ml]
EDW-1	15.5	3.8	22.0	96.5	38.7
EDW-2	15.5	3.8	22.1	76.5	38.6
EDW-3	15.4	3.8	22.7	58.9	39.7

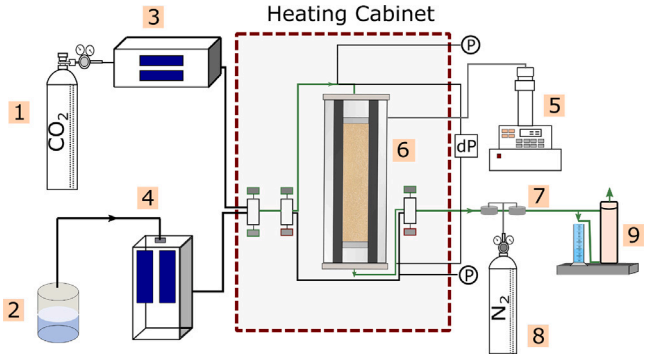

Fig. 1. Experimental setup used during the calcite dissolution experiments: Each core was wrapped in nickel foil to avoid CO_2 radial diffusion into the rubber sleeve of the core holder, and mounted vertically within a heating cabinet. 1 - CO_2 bottle, 2 - Aqueous phase, 3 - Quizix 6000-10k pump for CO_2 injection, 4 - Quizix 5000-10k pump for surfactant solution injection, 5 - Isco pump for confinement pressure, 6 - Hassler-type core holder with core, 7 - Equilibar backpressure regulator (BPR), 8 - N_2 bottle, 9 - adsorption column and measuring cylinder. The confining pressure was set to 21 MPa. The surfactant solutions were injected into the core from the top, and the two Equilibar backpressure regulators (BPR) connected to a nitrogen gas (N_2) tank maintained a constant system pressure.

after drying them for 2 weeks in a heating cabinet at 60 °C. The porosity (ϕ) values of each core were determined gravimetrically by air evacuating and saturating the cores with NaCl, NFB, and CB brines. The absolute brine permeability (k_0) was calculated using Darcy's law at different flow rates (50 ml/h to 200 ml/h). Edwards Limestone core properties are presented in Table 3.

2.3. Core flooding experiments

Induced carbonated dissolution was studied by steady CO_2 and surfactant solutions co-injection using the experimental setup presented in Fig. 1. The experiments were performed using a CO_2 fraction of 30% of the total volume injected, temperature, and pressure set to 40 °C and 18 MPa. Continuous recordings of dynamic changes in differential pressure were made in cores EDW-1 ($NaCl_{foam}$), EDW-2 (NFB_{foam}), and EDW-3 (CB_{foam}) and could indicate the creation (injection pressure reduction) or blockage (injection pressure increase) of flow paths in the porous medium.

2.4. Isothermal titration calorimetry

A multichannel microcalorimetric TAM IV system from TA Instruments was used to determine the rock-fluid-foam interactions that take place when a brine with surfactant and saturated with CO_2 is injected into Edwards Limestone wetted with the same brine. The microcalorimeter unit has a precision of ± 100 nW and a long-term

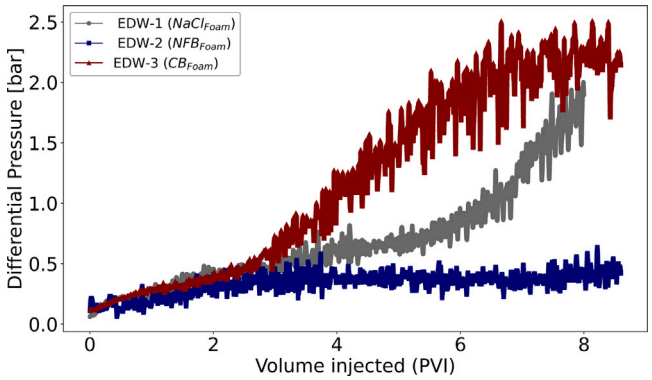

Fig. 2. Differential pressure (DP) development for EDW-1 ($NaCl_{foam}$), EDW-2 (NFB_{foam}), and EDW-3 (CB_{foam}) core plugs.

stability of ±100 μ°C/24 h (TA instruments, 2015). As mentioned in a previous work (Cobos et al., 2018), Isothermal Titration Calorimetry (ITC) is a direct appraisal of the thermodynamics behind complex processes since it is the only method that measures directly enthalpy change (ΔH) of a binding interaction. Consequently, it offers a higher degree of accuracy compared to other methods (e.g. van't Hoff method) that estimate the enthalpy change based on theoretical computations. Moreover, the ITC results are comparable to the core floods since the Gibbs free energy (ΔG) of a chemical reaction is almost independent of pressure (Cobos et al., 2023). The ITC experiments were performed using ampules containing a slurry of 100 mg Edwards Limestone and 200 μL of one of the brines (NaCl, NFB, CB) at ambient temperature and pressure conditions. After 1 h of equilibrium time at 40 °C, seven injections of 9.948 μL of the selected foam formulation were titrated with a time interval of 420 s into the brine-wetted rock particles. Note that a set temperature and interactions with only one surfactant are the main limitations for the microcalorimetric evaluation presented in this work. $NanoAnalyze^{TM}$ software from TA Instruments was used to analyze the ITC experiments.

3. Results

3.1. Darcy-scale investigations

The development in differential pressures (DP) during continuous co-injection of sc-CO_2 and different surfactant solution formulations (NaCl, NFB, CB) into cores EDW-1, EDW-2, and EDW-3 is presented in Fig. 2. The displacement of the foams in the porous medium resulted in a differential pressure increase, which can indicate the blockage of pores or flow paths due to dissolution/precipitation reactions. (Cobos et al., 2023) also observed a similar trend for the co-injection of sc-CO_2 and NaCl brine without surfactant into Edwards Limestone. Those authors obtained 0.28 bars DP during the continuous co-injection of sc-CO_2 and NaCl brine without surfactant. In the present study, the $NaCl_{foam}$ injection attains 2 bars DP. The observed difference between the two co-injections with NaCl may be attributable to the in-situ foam generation and propagation in the case of $NaCl_{foam}$.

The porosity of the core plugs was measured before and after the flooding experiment, which increased from 22.0% to 31.6% (EDW-1), 22.1% to 23.8% (EDW-2), and 22.7% to 23.36% (EDW-3). Fig. 3 presents the non-continuous calcite dissolution with the formation of highly conductive channels known as 'wormholes' for EDW-3 after the coreflooding experiments. Note that EDW-3 flooded with CB_{foam} was the most brittle core plug among the other two cores (EDW-1 and EDW-2).

Several authors (Noiriel et al., 2009; de Freitas Filho, 2012; Lamy-Chappuis et al., 2014; Ribeiro et al., 2016; Rembert et al., 2022)

Fig. 3. EDW-3 core plug after CB_{foam} injection.

reported changes in porosity and permeability in carbonate rocks due to dissolution/precipitation reactions. Noiriel et al. (2009) observed a porosity increase from 20.3 to 30.2% in a Limestone sample during a flow-through experiment using CO_2 rich water with the aid of X-ray micro-tomography. The authors mentioned that the porosity increase was slightly higher near the inlet and not evenly distributed through the Limestone sample. Similar results were found by Lamy-Chappuis et al. (2014) in core flooding experiments using calcite-riched sandstone cores for 58 h. Those authors observed that half the porosity increase occurred during the first 3 h and 90% within 18 h. Porosity changes could compromise the reservoir integrity with subsequent surface subsidence since the rock's stiffness and strength are strongly related to its porosity. Porosity changes could impact the structural integrity of a reservoir, posing risks not only to the reservoir itself but also to the environment (e.g. upwards CO_2 leakage) (Bonto et al., 2021). Nevertheless, the severity of the porosity changes due to dissolution/precipitation reactions at the field scale may be less than what was observed in the experimental studies (Zareei et al., 2022).

3.2. Micro-scale investigation

The previous Darcy-Scale investigations showed that Edwards Limestone reacted differently with the different foam formulations (same surfactant but different ionic composition). Consequently, further investigations at a micro-scale will be presented in this section.

Rock-fluid-foam and fluid-foam interactions were measured on the micro-scale using calorimetry. The raw heat signal registered by the TAM IV microcalorimeter for the rock-fluid-foam interactions is presented in Fig. 4.

Each peak in the thermograms (Fig. 4) corresponds to endothermic events. The data collection of the microcalorimeter apparatus indicates that negative peaks are associated with endothermic processes, which are observed when a foam made of NaCl, NFB, or CB brines contacts the rock+fluid system. In other words, the interaction between NaCl, NFB, or CB foams and the rock+fluid systems is endothermic. Note that each peak in all the thermograms indicates the addition of 9.947 μL of each foam formulation into the rock+fluid systems.

Fluid-foam interactions were also performed to distinguish the impact of the ionic composition in the CO_2 foam behavior. The thermogram of the interaction between each foam formulation ($NaCl_{foam}$, NFB_{foam}, CB_{foam}) and the same fluid is presented in Fig. 5.

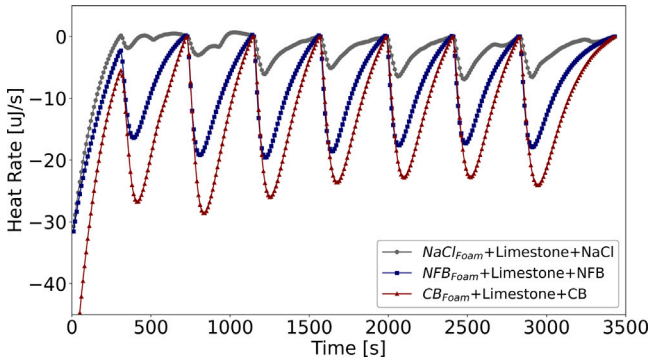

Fig. 4. Heat flow vs. time for $NaCl_{foam}$, NFB_{foam} and CB_{foam} systems.

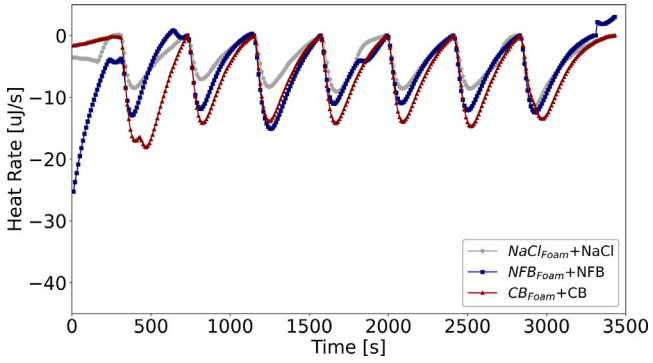

Fig. 5. Heat flow vs. time for $NaCl_{foam}$, NFB_{foam}, and CB_{foam} into either NaCl, NFB or CB.

The integration of the heat rate displayed in Figs. 4–5 over time gives the heat developed Q_{inj} by the injection of each foam formulation into either the rock-fluid-foam or fluid-foam systems. Table 4 shows the heat values for each foam system. The total adsorbed heat (H_T) in the rock-fluid-foam systems are 6.9 mJ $NaCl_{foam}$, 19.3 mJ NFB_{foam}, and 37.8 mJ CB_{foam} systems. On the other hand, the total heat for the fluid-foam interactions (H_{fl-fm}) are 11.5 mJ $NaCl_{foam}$, 12.5 NFB_{foam}, and 20.4 mJ CB_{foam}, respectively. Both rock-fluid-foam and fluid-foam interactions show that CB_{foam} requires more energy than the other foams and might be associated with processes that require energy to proceed (micelle formation or rock dissolution)

The data presented in Table 4 can be used to calculate the enthalpy change per unit ionic strength (ΔH) for the rock-fluid-foam and fluid-foam interactions through Eq. (1). This is because the heat of those interactions is equal to the enthalpy change (ΔH) at isobaric and isothermal conditions as explained in Cobos et al. (2018). In this equation, [IS] is the ionic strength of one of the brines (NaCl, NFB, CB) in mmol/L, and V_{inj} is the volume of each titration.

$$Q_{inj} = \left(\Delta H \times [IS] \times V_{inj}\right) \quad (1)$$

The enthalpy change (ΔH) for the rock-fluid-foam interaction of the three foaming systems is displayed in Fig. 6. As revealed, the CB_{foam} attains the highest interaction, which could be associated with calcite dissolution as observed previously in the core flooding experiments.

Fig. 7 shows the enthalpy change (ΔH) for the fluid-foam interactions. The enthalpy change for all the fluid-foam systems is higher than for the rock-fluid-foam systems (see. Fig. 6). It could be associated with a micelle formation process, which is an entropy-driven process.

Several authors (Paula et al., 1995; Opatowski et al., 2002; Shi et al., 2019; Spiering et al., 2021) also found through experimental and simulation work that the micelle formation of non-ionic surfactants is

Table 4
Heat values for $NaCl_{foam}$, NFB_{foam}, and CB_{foam} systems.

inj no.	$NaCl_{foam}$		NFB_{foam}		CB_{foam}	
	H_T (mJ)	H_{fl-fm} (mJ)	H_T (mJ)	H_{fl-fm} (mJ)	H_T (mJ)	H_{fl-fm} (mJ)
1	0.13 ± 0.01	1.32 ± 0.44	2.72 ± 0.39	1.91 ± 0.44	5.69 ± 0.17	3.78 ± 0.63
2	0.22 ± 0.10	1.25 ± 0.12	2.80 ± 0.53	1.81 ± 0.08	5.85 ± 0.29	2.56 ± 0.16
3	0.69 ± 0.30	1.46 ± 0.26	3.09 ± 0.42	1.82 ± 0.04	5.44 ± 0.19	2.70 ± 0.05
4	1.02 ± 0.23	1.07 ± 0.58	2.55 ± 0.49	1.96 ± 0.02	5.07 ± 0.08	2.59 ± 0.23
5	1.21 ± 0.20	1.65 ± 0.18	2.49 ± 0.45	1.96 ± 0.03	4.89 ± 0.09	2.78 ± 0.02
6	1.29 ± 0.16	1.87 ± 0.03	2.57 ± 0.41	1.45 ± 0.36	4.82 ± 0.15	2.69 ± 0.29
7	0.86 ± 0.39	2.92 ± 0.32	3.11 ± 0.53	1.61 ± 0.16	6.06 ± 0.29	3.33 ± 0.01

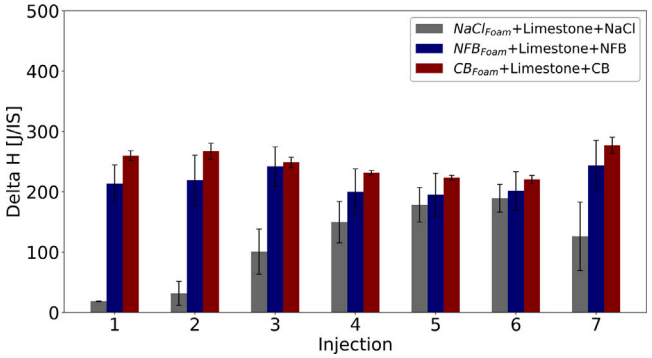

Fig. 6. Enthalpy change (ΔH) values for $NaCl_{foam}$, NFB_{foam} and CB_{foam} rock-fluid-foam systems. The error bars range from 0.6–56 mJ $NaCl_{foam}$, 30–41 mJ NFB_{foam}, and 3–13 mJ CB_{foam}.

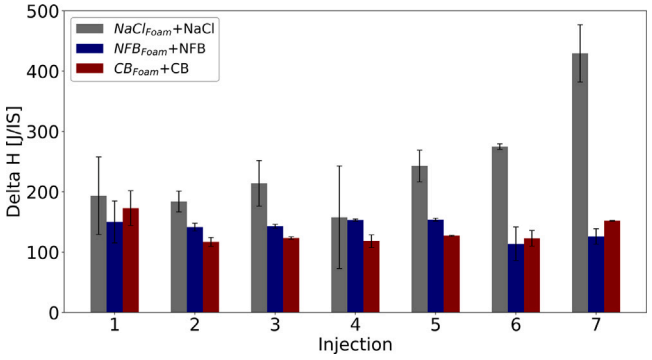

Fig. 7. Enthalpy change (ΔH) values for $NaCl_{foam}$, NFB_{foam} and CB_{foam} injected into the corresponding pure brines. The error bars range from 5–84 mJ $NaCl_{foam}$, 2–34 mJ NFB_{foam}, and 0.6–28 mJ CB_{foam}.

endothermic at low temperatures (25–50 °C). Those authors explained that the energy required to break the hydrogen bonds between water molecules and the surfactant head groups is greater than the energy released by the aggregation of the hydrophobic tails. Spiering et al. (2021) reported through calorimetry that the enthalpy for the micelle formation of a tailor-made non-ionic surfactant ($C_{12}EO_{14}-OH$) is 9.4 kJ/mol at 40 °C. Surfonic L24-22 has a hydrophilic-CO_2 philic balance (HCB) equal to 16.6. Consequently, this surfactant prefers the water phase and could form micelles. The concentration of Surfonic L24-22 in all the experiments was 0.5 w% which is expected to be above the critical micelle formation concentration (CMC). As observed in Fig. 7, $NaCl_{foam}$ is more endothermic than the other foam formulations (NFB_{foam} and CB_{foam}). This could indicate that the trend for the formation of stable micelles follows: CB_{foam}<NFB_{foam}<$NaCl_{foam}$. Consequently, more micelles are formed in each $NaCl_{foam}$ injection into NaCl.

As shown in the core flooding experiments, the injection of CO_2 foams ($NaCl_{foam}$, NFB_{foam}, CB_{foam}) resulted in the dissolution of Edwards Limestone. Consequently, it is important to determine the direct

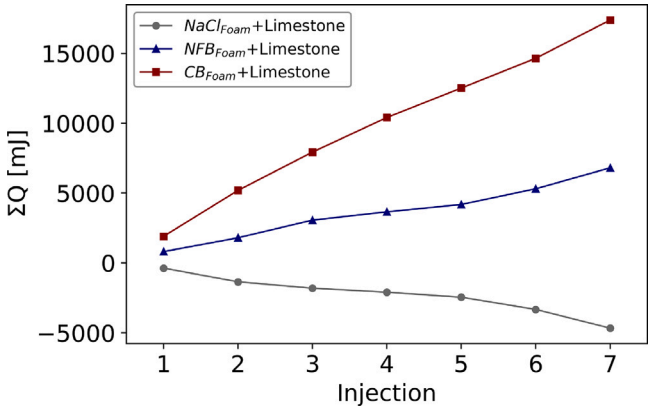

Fig. 8. Cumulative Heat response of foams interaction with Edwards Limestone. The error bars range from 5–84 mJ $NaCl_{foam}$, 2–34 mJ NFB_{foam}, and 0.6–28 mJ CB_{foam}.

rock-foam interactions. The strategy used to determine the interaction between the foam formulations and Edwards Limestone is the following according to Eq. (2). The total heat (H_T) is comprised of the heat of interaction between the rock-fluid-foam ($H_{r-fl-fm}$) and fluid-foam (H_{fl-fm}). It is possible to get a value for the interaction between rock and foam formulation by subtracting the fluid-foam interaction heat (H_{fl-fm}) from the total heat (see. Eq. (2)). In the mentioned equation, (T) is total interaction, (r) corresponds to Limestone particles, (fl) is one of the fluids (NaCl, NFB, CB), (fm) corresponds to a foam formulation ($NaCl_{foam}$, NFB_{foam}, CB_{foam}). Note that this calculation was done because rock-foam interaction could not be measured directly; the heat of evaporation of the tested solutions masks the real effect at 40 °C.

$$H_{r-fm} = H_T - H_{fl-fm} \quad (2)$$

Fig. 8 shows the cumulative heat of adsorption, ΣQ (mJ), for the interaction between the foam formulations and Edwards Limestone. As observed both CB_{foam} and NFB_{foam} injected into Edwards Limestone are endothermic reactions, whereas, $NaCl_{foam}$ is exothermic. Notice that the heat response for $NaCl_{foam}$ is mainly determined by the fluid-foam interactions (see. Figs. 6–7).

The endothermicity of both CB_{foam} and NFB_{foam} could indicate demicellization when the foam formulations contact the rock lattice, which could lead to calcite dissolution. In the case of pure brine-rock interaction, the incorporation of Ca^{2+} and Mg^{2+} ions as inner-sphere complexes into the atomic structure of calcite are exothermic (Cobos and Søgaard, 2021). Consequently, the endothermicity of both CB_{foam} and NFB_{foam} could indicate demicellization when the foam formulations contact the rock lattice, thus leading to calcite dissolution. Cobos et al. (2023) also reported that calcite dissolution is an endothermic process, which is driven by the increase of cations and hydrogen carbonate concentrations in the brine upon dissolution (entropy change). It is believed that the trapped CO_2 could have been released when the micelle are broken. Consequently, CO_2 that was previously encapsulated could have formed carbonic acid (H_2CO_3) that subsequently

dissociates into H^+ and bicarbonate ions when dissolved in water and they attacked the rock. The demicellization process involves changes in the hydration of the head groups and the counterions, which is larger for CB_{foam} and NFB_{foam}. Both foam formulations are composed of divalent ions (Ca^{2+}, Mg^{2+}) that tend to be more strongly hydrated than monovalent Na^+ ions because of their higher ionic potential (charged divided by size is higher). The $NaCl_{foam}$ micelles, on the other hand, are more stable, and therefore less calcite dissolution is expected. Calcite dissolution and wormhole formation due to CO_2 foam injection in carbonates have been also observed by Gland et al. (2018), Jian et al. (2020), and Jones et al. (2022). The dissolution of the rock begins at the core inlet and extends towards the inlet surface (approximately half-length of the core) Jian et al. (2020). According to Jones et al. (2022)), several small holes are formed at the beginning of the CO_2 foam injection. One of those holes will become slightly more dominant and thereafter it will turn into the main flow path into the rock and dissolution will then continue along this preferential path (growing wormhole). The importance of these wormholes is underscored when considering their application in carbon storage and enhanced oil recovery since they can be either beneficial or detrimental. Wormholing can potentially improve well injectivity by creating flow conduits in the reservoir. This can enhance the movement of fluids within the reservoir and, therefore, improve the distribution of CO_2 that leads to better crude oil displacement and recovery. On the other hand, it could compromise the structural integrity of the well due to a localized dissolution (Snippe et al., 2020). As mentioned by Rossen et al. (2022), additional research is required to quantify this problem and to devise solutions to address it. Moreover, the implementation of foam-assisted CO_2 sequestration includes optimizing surfactant performance and stability, while further reducing cost and adsorption. The financial aspect of implementing foam for CO_2 sequestration is heavily influenced by the cost of chemicals. Any decrease in the cost of these chemicals would subsequently lower the overall expense of the sequestration process.

4. Conclusions

This work presented an evaluation of induced calcite dissolution using foam formulations with a different ionic composition. Based on the experimental results at darcy- and micro-scales, the overall conclusions are summarized as follows:

- The differential pressures (DP) development during the first 8 PVI for the Limestone core plugs (EDW-1, EDW-1, and EDW-3) flooded with different CO_2 foam formulations shows that CB_{foam} attains the highest pressure drop due to dissolution/precipitations processes. It was observed that EDW-3 was much more brittle than the other core plugs
- The steady-state co-injection of $NaCl_{foam}$, NFB_{foam}, and CB_{foam} causes a non-continuous dissolution of Edwards Limestone and a porosity increase in all the Limestone core plugs (EDW-1, EDW-1, and EDW-3) due to the formation of highly conductive channels known as wormholes
- The heat absorbed by CB_{foam} is higher than for NFB_{foam} and $NaCl_{foam}$ into Edwards Limestone wetted with a similar brine. This could be related to calcite dissolution that was observed in the core flooding experiments
- Fluid-foam experiments indicate the formation of micelles, which is an endothermic process driven by entropy. The trend for the formation of those stable micelles follows: $CB_{foam} < NFB_{foam} < NaCl_{foam}$
- Rock-foam interactions that were calculated based on the total rock-fluid-foam and fluid-foam interactions showed that the process with both NFB_{foam} and CB_{foam} are endothermic, which could be related to the demicellization of the micelles. This process could lead to calcite dissolution due to the release of encapsulated CO_2 that could dissolve in water and form carbonic acid that subsequently dissociates into H^+ and bicarbonate ions (HCO_3^-). Those ions are responsible for the observed calcite dissolution.

Nomenclature

ϕ	Porosity
ΔH	Enthalpy change
BPR	Back pressure regulator
CCS	Carbon Capture and Storage
d	Diameter
EOR	Enhanced Oil Recovery
f_g	Gas fraction
HCB	Hydrophilic-CO_2 philic balance
ITC	Isothermal Titration Calorimetry
IS	Ionic strength
k_0	Initial permeability
l	Length
P	Pressure
PV	Pore volume
PVI	Pore volumes injected
V_{inj}	Volume injected

CRediT authorship contribution statement

Jacquelin E. Cobos: Writing – review & editing, Writing – original draft, Methodology, Investigation, Formal analysis, Data curation. **Aleksandra M. Sæle:** Methodology, Investigation. **Maria C. Benjumea:** Methodology, Investigation. **Monica M. Charro:** Methodology, Investigation. **Erik G. Søgaard:** Writing – review & editing, Supervision, Investigation, Conceptualization.

Declaration of competing interest

The authors declare that they have no known competing financial interests or personal relationships that could have appeared to influence the work reported in this paper.

Data availability

Data will be made available on request.

Acknowledgments

The authors would like to thank the Norwegian Agency for Development Cooperation (NORAD) under grant 71660 for financial support.

References

Al-Khdheeawi, E.A., Vialle, S., Barifcani, A., Sarmadivaleh, M., Iglauer, S., 2018. Enhancement of CO_2 trapping efficiency in heterogeneous reservoirs by water-alternating gas injection. Greenh Gases: Sci. Technol. 8 (5), 920–931.

Alcorn, Z.P., Føyen, T., Zhang, L., Karakas, M., Biswal, S.L., Hirasaki, G., Graue, A., 2020. CO_2 foam field pilot design and initial results. SPE Improved Oil Recovery Conference, vol. Day 1 Mon, August 31, 2020, D011S007R003, URL https://doi.org/10.2118/200450-MS.

Alcorn, Z.P., Fredriksen, S.B., Sharma, M., Rognmo, A.U., Føyen, T.L., Fernø, M.A., Graue, A., 2019. An integrated carbon-dioxide-foam enhanced-oil-recovery pilot program with combined carbon capture, utilization, and storage in an onshore texas heterogeneous carbonate field. SPE Reserv. Eval. Eng. 22 (04), 1449–1466, URL https://doi.org/10.2118/190204-PA.

Anabaraonye, B.U., Crawshaw, J.P., Trusler, J.M., 2019. Brine chemistry effects in calcite dissolution kinetics at reservoir conditions. Chem. Geol. 509, 92–102, URL https://www.sciencedirect.com/science/article/pii/S0009254119300099.

Aspenes, E., Graue, A., Ramsdal, J., 2003. In situ wettability distribution and wetting stability in outcrop chalk aged in crude oil. J. Pet. Sci. Eng. 39 (3), 337–350, URL https://www.sciencedirect.com/science/article/pii/S0920410503000731, Reservoir Wettability.

Bonto, M., Welch, M., Lüthje, M., Andersen, S., Veshareh, M., Amour, F., Afrough, A., Mokhtari, R., Hajiabadi, M., Alizadeh, M., Larsen, C., Nick, H., 2021. Challenges and enablers for large-scale CO_2 storage in chalk formations. Earth-Sci. Rev. 222, 103826, URL https://doi.org/10.1016/j.earscirev.2021.103826.

Calabrese, M., Masserano, F., Blunt, M.J., 2005. Simulation of physical-chemical processes during carbon dioxide sequestration in geological structures. SPE Annual Technical Conference and Exhibition, vol. All Days, pp. SPE–95820–MS, URL https://doi.org/10.2118/95820-MS.

Cobos, J.E., Folkvord, O.P., Søgaard, E.G., Brattekås, B., 2023. Microscopic and macroscopic assessment of carbonate dissolution for geologic CO_2 storage. Discov. Energy 3, URL https://doi.org/10.1007/s43937-023-00017-1.

Cobos, J.E., Sandnes, M., Steinsbø, M., Brattekås, B., Søgaard, E.G., Graue, A., 2021. Evaluation of wettability alteration in heterogeneous limestone at microscopic and macroscopic levels. J. Pet. Sci. Eng. 202, 108534, URL https://doi.org/10.1016/j.petrol.2021.108534.

Cobos, J.E., Søgaard, E.G., 2021. Effect of individual ions on rock-brine-oil interactions: A microcalorimetric approach. Fuel 290, 119955, URL https://doi.org/10.1016/j.fuel.2020.119955.

Cobos, J.E., Westh, P., Søgaard, E.G., 2018. Isothermal titration calorimetry study of brine oil rock interactions. Energy & Fuels 32 (7), 7338–7346, URL https://doi.org/10.1021/acs.energyfuels.8b00512.

Crockford, P., Telmer, K., Best, M., 2014. Dissolution kinetics of devonian carbonates at circum-neutral pH, 50 bar pCO_2, 105°C, and 0.4M: The importance of complex brine chemistry on reaction rates. Appl. Geochem. 41, 128–134, URL https://doi.org/10.1016/j.apgeochem.2013.12.008.

de Freitas Filho, R.D., 2012. Effects of dissolution on the permeability and porosity of limestone and dolomite in high pressure CO_2/water systems. SPE Annual Technical Conference and Exhibition, vol. All Days, pp. SPE–160911–STU, URL https://doi.org/10.2118/160911-STU.

Dong, P., Puerto, M., Jian, G., Ma, K., Mateen, K., Ren, G., Bourdarot, G., Morel, D., Bourrel, M., Biswal, S.L., Hirasaki, G., 2018. Low-IFT foaming system for enhanced oil recovery in highly heterogeneous/fractured oil-wet carbonate reservoirs. SPE J. 23 (06), 2243–2259, URL https://doi.org/10.2118/184569-PA.

Eiken, O., Ringrose, P., Hermanrud, C., Nazarian, B., Torp, T.A., Høier, L., 2011. Lessons learned from 14 years of CCS operations: Sleipner, in Salah and Snøhvit. Energy Procedia 4, 5541–5548.

Ellis, B., Peters, C., Fitts, J., Bromhal, G., McIntyre, D., Warzinski, R., Rosenbaum, E., 2011. Deterioration of a fractured carbonate caprock exposed to CO_2-acidified brine flow. Greenh. Gases: Sci. Technol. 1 (3), 248–260, URL https://doi.org/10.1002/ghg.25.

Enick, R.M., Olsen, D., Ammer, J., Schuller, W., 2012. Mobility and conformance control for CO_2 EOR via thickeners, foams, and gels - A literature review of 40 years of research and pilot tests. SPE Improved Oil Recovery Conference, vol. All Days, URL https://doi.org/10.2118/154122-MS.

Farajzadeh, R., Lotfollahi, M., Eftekhari, A.A., Rossen, W.R., Hirasaki, G.J.H., 2015. Effect of permeability on implicit-texture foam model parameters and the limiting capillary pressure. Energy Fuels 29 (5), 3011–3018, URL https://doi.org/10.1021/acs.energyfuels.5b00248.

Føyen, T.L., 2020. CO_2 foam using non-ionic surfactants : For increased storage capacity and oil recovery.

Føyen, T., Brattekås, B., Fernø, M., Barrabino, A., Holt, T., 2020. Increased CO_2 storage capacity using CO_2-foam. Int. J. Greenh. Gas Control 96, 103016, URL https://www.sciencedirect.com/science/article/pii/S1750583619307558.

Gland, N., Chevallier, E., Cuenca, A., Batot, G., 2018. New developement of cationic surfactant formulations for foam assisted CO_2-EOR in carbonates formations. Abu Dhabi International Petroleum Exhibition and Conference, vol. Day 3 Wed, November 14, 2018, D031S089R003, URL https://doi.org/10.2118/193201-MS.

Heeschen, K., Risse, A., Ostertag-Henning, C., Stadler, S., 2011. Importance of co-captured gases in the underground storage of CO_2 : Quantification of mineral alterations in chemical experiments. Energy Procedia 4, 4480–4486, URL https://doi.org/10.1016/j.egypro.2011.02.403, 10th International Conference on Greenhouse Gas Control Technologies.

Hoefner, M.L., Evans, E.M., 1995. CO_2 foam: Results from four developmental field trials. SPE Reserv. Eng. 10 (04), 273–281, URL https://doi.org/10.2118/27787-PA.

International Energy Agency, 2015. Storing CO_2 through Enhanced Oil Recovery. OECD/IEA 2015.

Jian, G., Alcorn, Z., Zhang, L., Puerto, M.C., Soroush, S., Graue, A., Biswal, S.L., Hirasaki, G.J., 2020. Evaluation of a nonionic surfactant foam for CO_2 mobility control in a heterogeneous carbonate reservoir. SPE J. (Soc. Petrol. Eng. (U.S.) : 1996) 25 (6), 3481–3493.

Jian, G., Zhang, L., Da, C., Puerto, M., Johnston, K.P., Biswal, S.L., Hirasaki, G.J., 2019. Evaluating the transport behavior of CO_2 foam in the presence of crude oil under high-temperature and high-salinity conditions for carbonate reservoirs. Energy & Fuels 33 (7), 6038–6047. http://dx.doi.org/10.1021/acs.energyfuels.9b00667.

Jones, S.A., Kahrobaei, S., van Wageningen, N., Farajzadeh, R., 2022. CO_2 foam behavior in carbonate rock: Effect of surfactant type and concentration. Ind. Eng. Chem. Res. 61 (32), 11977–11987, URL https://doi.org/10.1021/acs.iecr.2c01186.

Lamy-Chappuis, B., Angus, D., Fisher, Q., Grattoni, C., Yardley, B.W.D., 2014. Rapid porosity and permeability changes of calcareous sandstone due to CO_2-enriched brine injection. Geophys. Res. Lett. 41 (2), 399–406.

Liu, Y., Grigg, R.B., Svec, R.K., 2005. CO_2 foam behavior: Influence of temperature, pressure, and concentration of surfactant. SPE Oklahoma City Oil and Gas Symposium / Production and Operations Symposium, vol. All Days, URL https://doi.org/10.2118/94307-MS.

Núñez López, V., Gil-Egui, R., Hosseini, S.A., 2019. Environmental and operational performance of CO_2-EOR as a CCUS technology: A cranfield example with dynamic LCA considerations. Energies 12 (3), http://dx.doi.org/10.3390/en12030448.

Luquot, L., Gouze, P., 2009. Experimental determination of porosity and permeability changes induced by injection of CO_2 into carbonate rocks. Chem. Geol. 265 (1), 148–159, URL https://doi.org/10.1016/j.chemgeo.2009.03.028.

Metz, B., Davidson, O., De Coninck, H., Loos, M., Meyer, L., 2005. IPCC Special Report on Carbon Dioxide Capture and Storage. Intergovernmental Panel on Climate Change, Cambridge University Press.

Motie, M., Assareh, M., 2020. CO_2 sequestration using carbonated water injection in depleted naturally fractured reservoirs: A simulation study. Int. J. Greenh. Gas Control 93, 102893, URL https://doi.org/10.1016/j.ijggc.2019.102893.

Noiriel, C., Luquot, L., Made, B., Raimbault, L., Gouze, P., van der Lee, J., 2009. Changes in Reactive Surface Area during limestone dissolution: An experimental and modelling study. Chem. Geol. 265 (1–2), 160–170.

Opatowski, E., Kozlov, M.M., Pinchuk, I., Lichtenberg, D., 2002. Heat evolution of micelle formation, dependence of enthalpy, and heat capacity on the surfactant chain length and head group. J. Colloid Interface Sci. 246 (2), 380–386. http://dx.doi.org/10.1006/jcis.2001.8050.

Orr, Jr., F.M., 2018. Carbon capture, utilization, and storage: An update. SPE J. 23 (06), 2444–2455. http://dx.doi.org/10.2118/194190-PA.

Ozaki, M., Nakazawa, N., Omata, A., Komatsu, M., Manabe, H., 2015. Ship-based carbon dioxide capture and storage for enhanced oil recovery. In: OTC Offshore Technology Conference. http://dx.doi.org/10.4043/25861-MS.

Paula, S., Sues, W., Tuchtenhagen, J., Blume, A., 1995. Thermodynamics of micelle formation as a function of temperature: A high sensitivity titration calorimetry study. J. Phys. Chem. 99 (30), 11742–11751, URL https://doi.org/10.1021/j100030a019.

Peng, C., Anabaraonye, B.U., Crawshaw, J.P., Maitland, G.C., Trusler, J.P.M., 2016. Kinetics of carbonate mineral dissolution in CO_2-acidified brines at storage reservoir conditions. Faraday Discuss. 192, 545–560, URL http://dx.doi.org/10.1039/C6FD00048G.

Pokrovsky, O.S., Golubev, S.V., Schott, J., 2005. Dissolution kinetics of calcite, dolomite and magnesite at 25°c and 0 to 50 atm p CO_2. Chem. Geol. 217 (3), 239–255, URL https://www.sciencedirect.com/science/article/pii/S000925410500015X.

Rembert, F., Jougnot, D., Luquot, L., Guérin, R., 2022. Interpreting self-potential signal during reactive transport: Application to calcite dissolution and precipitation. Water 14 (10), 1632.

Ribeiro, A.S., Mackay, E.J., Guimarães, L., 2016. Predicting calcite scaling risk due to dissolution and re-precipitation in carbonate reservoirs during CO_2 injection. SPE International Oilfield Scale Conference and Exhibition, vol. All Days, pp. SPE–179884–MS. http://dx.doi.org/10.2118/179884-MS.

Riding, J., Rochelle, C., 2005. The IEA Weyburn CO_2 Monitoring and Storage Project. British Geological Survey.

Rossen, W.R., Farajzadeh, R., Hirasaki, G.J., Amirmoshiri, M., 2022. Potential and challenges of foam-assisted CO_2 sequestration. SPE Improved Oil Recovery Conference, D021S014R001. http://dx.doi.org/10.2118/209371-MS.

Shi, P., Zhang, H., Lin, L., Song, C., Chen, Q., Li, Z., 2019. Molecular dynamics simulation of four typical surfactants in aqueous solution. RSC Adv. 9 (6), 3224–3231.

Snippe, J., Berg, S., Ganga, K., Brussee, N., Gdanski, R., 2020. Experimental and numerical investigation of wormholing during CO_2 storage and water alternating gas injection. Int. J. Greenh. Gas Control 94, 102901, URL https://doi.org/10.1016/j.ijggc.2019.102901.

Spiering, V.J., Lutzki, J., Gradzielski, M., 2021. Thermodynamics of micellization of nonionic surfactants – The effect of incorporating CO_2 moieties into the head group. J. Colloid Interface Sci. 581, 794–805.

TA instruments, 2015. TAM IV from TA instruments.

Tipura, L., 2008. Wettability Characterization by NMR T_2 Measurements in Edwards Limestone (Master's thesis). University of Bergen, Department of Physics and Technology.

Zareei, D., Rostami, B., Kostarelos, K., 2022. Petrophysical changes of carbonate rock related to CO_2 injection and sequestration. Int. J. Greenh. Gas Control 117, 103648, URL https://doi.org/10.1016/j.ijggc.2022.103648.